Report Title: "Synthesis and characterization of new intermetallic compounds" for the grant entitled "Laser processing of advanced magnetic materials"

Type of Report: Semi-Annual

Reporting Period Start Date: September 12, 2002

Reporting Period End Date: March 11, 2003

Principal Author: Professor Monica Sorescu

Date Report was Issued: May 7, 2003

DOE Award Number: DE-FC26-02NT41595

Name and Address of Submitting Organization: Duquesne University, Bayer School of Natural and Environmental Sciences, Department of Physics, Pittsburgh, PA 15282-0321

DISCLAIMER

ABSTRACT

This six-month work is focused mainly on the properties of novel magnetic intermetallics. In the first project, we synthesized several 2:17 intermetallic compounds, namely $Nd_2Fe_{15}Si_2$, $Nd_2Fe_{15}Al_2$, $Nd_2Fe_{15}SiAl$ and $Nd_2Fe_{15}SiMn$, as well as several 1:12 intermetallic compounds, such as $NdFe_{10}Si_2$, $NdFe_{10}Al_2$, $NdFe_{10}SiAl$ and $NdFe_{10}MnAl$. In the second project, seven compositions of $Nd_xFe_{100-x-y}B_y$ ribbons were prepared by a melt spinning method with Nd and B content increasing from 7.3 and 3.6 to 11 and 6, respectively. The alloys were annealed under optimized conditions to obtain a composite material consisting of the hard magnetic $Nd_2Fe_{14}B$ and soft magnetic α-Fe phases, typical of a spring magnet structure. In the third project, intermetallic compounds of the type $Zr_1Cr_1Fe_1T_{0.8}$ with T=Al, Co and Fe were subjected to hydrogenation. In the fourth project, we performed three crucial experiments. In the first experiment, we subjected a mixture of Fe_3O_4 and Fe (80-20 wt %) to mechanochemical activation by high-energy ball milling, for time periods ranging from 0.5 to 14 hours. In the second experiment, we ball-milled Fe_3O_4:Co^{2+} (x=0.1) for time intervals between 2.5 and 17.5 hours. Finally, we exposed a mixture of Fe_3O_4 and Co (80-20 wt %) to mechanochemical activation for time periods ranging from 0.5 to 10 hours. In all cases, the structural and magnetic properties of the systems involved were elucidated by X-ray diffraction (XRD), Mössbauer spectroscopy and hysteresis loop measurements. The four projects resulted in four papers, which are currently being considered for publication in Intermetallics, IEEE Transactions on Magnetics, Journal of Materials Science Letters and Journal of Materials Science. The contributions reveal for the first time in literature the effect of substitutions on the hyperfine magnetic field of neodymium-based intermetallics, the correlation between structure and magnetic properties in spring magnets, the unique effects induced by hydrogenation on the hyperfine parameters of iron-rich intermetallics and the characteristics of the ball milling process in systems containing magnetite.

TABLE OF CONTENTS

LIST OF GRAPHICAL MATERIAL

FIG. 1. Room-temperature transmission Mössbauer spectrum (a) and hyperfine magnetic field distribution (b) for $Nd_2Fe_{15}Si_2$ intermetallic compound.

FIG. 2. Room-temperature transmission Mössbauer spectra of $Nd_{11}Fe_{83}B_6$, $Nd_{10}DyFe_{83}B_6$ and $Nd_{10}Fe_{85}B_5$ systems.

FIG. 3. Room-temperature transmission Mössbauer spectrum of $Zr_1Cr_1Fe_1Al_{0.8}$ (a) before and (b) after hydrogenation.

FIG. 4. XRD spectra of $Fe_{3-x}Co_xO_4$ (x=0.1) exposed to ball milling for time periods ranging from 2.5 to 15 hours.

INTRODUCTION

Much attention has been focused during the past few years on the synthesis of iron-rare earth compounds with noncubic structures and high values of saturation magnetization and anisotropic field strength [1-8]. In particular, the 2:17 and 1:12 Nd-based intermetallics have attracted considerable interest as new materials for permanent magnet applications. Alloying substitutions in these systems are known to affect the Curie temperature, but their effect on the local magnetic fields is not yet understood. From this point of view, Mössbauer spectroscopy is able to provide detailed information on the hyperfine magnetic fields in these compounds. When dealing with substitutions, however, the number of nonequivalent positions increases significantly, such that a fit with a hyperfine magnetic fields distribution becomes a valid option [1]. This method is particularly suited when the average value of the hyperfine magnetic field is sought. In this project we obtain the hyperfine magnetic field distributions and average values of the hyperfine magnetic fields for several 2:17 and 1:12 Nd-based intermetallics and correlate the results with substitutional effects. Complementary information is obtained using XRD.

Nanocomposite magnetic materials consisting of a mixture of hard and soft magnetic phases are characterized by a combination of high magnetic remanence, high coercivity, high energy product and low cost [9, 10]. The enhancement of these magnetic properties is related to the exchange coupling between hard and soft nanograins.

In this work, the nanocomposite magnets with the hard magnetic $Nd_2Fe_{14}B$ and soft magnetic α-Fe phases are studied. They combine relatively high saturation magnetization with high remanence [11, 12]. Such nanocomposite structures can be obtained by proper annealing of some NdFeB-based alloys [12-15]. Our samples were prepared by annealing the melt-spun Nd-Fe-B ribbons having a wide range of compositions. The microstructure of the samples was

investigated by XRD and Mössbauer spectroscopy as a function of the alloy composition and annealing time and temperature. Mössbauer spectra allowed us to evaluate the relative amounts of the $Nd_2Fe_{14}B$ and α-Fe phases in the nanocomposite samples as well as all site populations. The influence of annealing conditions on the bulk magnetic properties is determined by measurement of the hysteresis loops.

In addition, the structure and magnetic properties of iron-rich intermetallics have attracted considerable interest due to their potential use as hydrogen storage materials [16-23]. However, the effect of hydrogenation on the hyperfine parameters of the Laves phases has not been studied to date. According to the current understanding of hydride formation mechanism in metals, a slight change in electronic makeup of a system which is caused by hydrogenation brings rather drastic changes in the magnetism of the system. Therefore, Mössbauer spectroscopy is an excellent probe to detect and understand the electronic structure of the host metals and their hydrides. We report in this work the results of a complete Mössbauer spectroscopy study at room and liquid helium temperatures of $Zr_1Cr_1Fe_1T_{0.8}$ and its hydrides, with T=Al, Co and Fe.

Finally, investigations of the magnetic properties of ball-milled materials are of great interest due to possible applications as permanent magnets, soft magnetic materials and in recording [24-28]. Ball milling has been introduced during the last few years as a powerful tool for the preparation of metastable crystalline and amorphous phases and nanostructured materials [29-31]. In particular, small particles of Fe_3O_4 embedded in a Cu matrix have been prepared by direct milling of a mixture of Cu and Fe_3O_4 powders [32]. It was shown that the most significant changes in phase composition, magnetization, coercivity, remanence and switching field distribution take place during the first 2 hours of milling.

In a different study, nanocrystalline Fe_3O_4 and a composite system constituted by nanocrystalline Fe and Fe_3O_4 have been synthesized by ball-milling commercial magnetite and

an equimolar mixture of iron and magnetite powders [33]. The presence of a sextet with anomalous hyperfine parameters in the Mössbauer spectrum of as-milled $Fe+Fe_3O_4$ has been associated with an alteration of the magnetite structure at the interface with bcc Fe. The magnetic properties of magnetite powder prepared by ball-milling of a stoichiometric mixture of hematite and iron were also reported [34-37]. Ball milling hematite with iron during periods ranging from 0.5 to 5 hours yielded magnetite with high magnetic hardness, characterized by coercive force three times higher than that typical for single-domain natural magnetites. In the present grant, we achieve mechanochemical activation of Fe_3O_4+Fe, Fe_3O_4:Co^{2+} and Fe_3O_4+Co for time periods ranging from 0.5 to 17.5 hours. The kinetics of phase transformation are studied by XRD and Mössbauer spectroscopy.

EXECUTIVE SUMMARY

In the first project, we synthesized several 2:17 intermetallic compounds, namely $Nd_2Fe_{15}Si_2$, $Nd_2Fe_{15}Al_2$, $Nd_2Fe_{15}SiAl$ and $Nd_2Fe_{15}SiMn$, as well as several 1:12 intermetallic compounds, such as $NdFe_{10}Si_2$, $NdFe_{10}Al_2$, $NdFe_{10}SiAl$ and $NdFe_{10}MnAl$. The substitutional effect on their magnetic properties was studied by Mössbauer spectroscopy using hyperfine magnetic field distributions. The structural properties of both classes of intermetallics were investigated using XRD. For both symmetries involved, it was found that Al and especially, Mn substitutions lower the value of the net magnetic moment, while Si additions correlate with high values of the average magnetic field and consequently, magnetic moment.

In the second project, seven compositions of $Nd_xFe_{100-x-y}B_y$ ribbons were prepared by a melt spinning method, with Nd and B content increasing from 7.3 and 3.6 to 11 and 6, respectively. The alloys were annealed under optimized conditions to obtain a composite material consisting of the hard magnetic $Nd_2Fe_{14}B$ and soft magnetic α-Fe phases, typical of a spring magnet structure. Phase analysis was performed by X-ray diffraction and Mössbauer spectroscopy, in order to obtain the hyperfine magnetic fields and site populations. In all alloys, the $Nd_2Fe_{14}B$ and α-Fe phases were formed due to annealing. However, in the case of $Nd_{11}Fe_{83}B_6$ alloy with the highest Nd content a significant amount of the $Nd_{1.1}Fe_4B_4$ paramagnetic phase was observed. In the studied set of alloys, the highest fraction of the α-Fe phase (about 30 %) was obtained for the $Nd_{7.3}Fe_{89.1}B_{3.6}$ alloy. The formation of the exchange coupled material was checked by hysteresis loop measurements at room temperature in all cases.

In the third project, intermetallic compounds of the type $Zr_1Cr_1Fe_1T_{0.8}$ with T=Al, Co and Fe were subjected to hydrogenation. The structural and magnetic properties of these intermetallic compounds and their hydrides were studied by Mössbauer spectroscopy at room and liquid helium temperatures. The effects observed to be induced by hydrogenation ranged from changes in site populations and onset of crystallographic disorder to enhancement of weak ferromagnetism in the compound with Fe.

In the fourth project, we performed three crucial experiments. In the first experiment, we subjected a mixture of Fe_3O_4 and Fe (80-20 wt %) to mechanochemical activation by high-energy ball milling, for time periods ranging from 0.5 to 14 hours. Complementary XRD and Mössbauer spectroscopy data demonstrated a phase transformation of magnetite to hematite, accompanied by a partial oxidation of iron to hematite. The reaction can be used to obtain nanometer-size magnetite by ball milling, due to the inhibition of its transformation to hematite, caused by the presence of iron atoms. In the second experiment, we ball-milled Fe_3O_4:Co^{2+} (x=0.1) for time intervals between 2.5 and 17.5 hours. Our XRD and Mössbauer measurements showed that the cobalt-doped magnetite undergoes a phase transformation to hematite, which is actually cobalt-doped hematite. We were able to show herewith that the Co ion is not kicked out of the lattice during the milling process, but undergoes the phase transformation inside the hematite lattice. Finally, we exposed a mixture of Fe_3O_4 and Co (80-20 wt %) to mechanochemical activation for time periods ranging from 0.5 to 10 hours. The XRD and Mössbauer results are consistent with the formation of cobalt ferrite (a strongly Co-substituted magnetite), with the occurrence of hematite as an intermediate product. In all three cases, the milling-induced phase transformations started with a considerable disorder of the octahedral sublattice of magnetite.

The four projects summarized here resulted in four papers, which are currently being considered for publication in Intermetallics, IEEE Transactions on Magnetics, Journal of Materials Science Letters and Journal of Materials Science. The first two papers have already been accepted for publication and are in press.

EXPERIMENTAL

The 2:17 and 1:12 Nd-based intermetallics were prepared by melting the components in an arc furnace under protective argon atmosphere. The ingots were turned several times to avoid inhomogeneities and annealed at 950-1050^{o}C for 10 days. XRD measurements were performed using a Rigaku D-2013 diffractometer with Cu $K_{\alpha 1}$ radiation at λ=1.5404 Å. Transmission Mössbauer measurements were made with a constant acceleration spectrometer. The 50 mCi gamma ray source was ^{57}Co in a Rh matrix, maintained at room temperature. All spectra were analyzed with the NORMOS-DIST program, which uses the histogram method to obtain the hyperfine magnetic field distributions.

The nanocomposite $Nd_2Fe_{14}B/\alpha$-Fe samples were prepared by annealing the melt-spun ribbons with seven different compositions of $Nd_{11}Fe_{83}B_6$, $Nd_{10}DyFe_{83}B_6$, $Nd_{10}Fe_{85}B_5$, $Nd_{9.3}Fe_{85.8}B_{4.9}$, $Nd_{8.5}Fe_{87.2}B_{4.3}$, $Nd_{7.9}Fe_{88.1}B_4$ and $Nd_{7.3}Fe_{89.1}B_{3.6}$. The optimized annealing conditions (time and temperature) were 15 minutes at 715^{o}C and/or 5 minutes at 726^{o}C and 750^{o}C. The crystallization products were identified by x-ray diffraction and Mössbauer spectroscopy. The Mössbauer spectra were recorded at room temperature using a source of ^{57}Co in Rh matrix. Hyperfine parameters and relative abundance of the phases formed were determined from the spectra. The relative phase abundance is defined as the relative area of the relevant subspectral components. Bulk magnetic properties of the Nd-Fe-B alloys were studied by measurement of the hysteresis loops at room temperature.

The samples of $Zr_1Cr_1Fe_1T_{0.8}$ with T=Al, Co and Fe were prepared by induction melting stoichiometric amounts of constituent elements in a water-cooled copper boat under a continuous flow of purified argon gas. The ingots were turned over and remelted several times to ensure homogeneity. Then, the compounds were annealed at 1000^{o}C for 3 h in the boat. X-ray diffraction patterns using Cu-Kα radiation with a graphite monochrometer revealed single phases

of the hexagonal Laves (C14 type) structures. To obtain crystal structural and magnetic data on the hydrides, the compounds were exposed to high purity hydrogen at a pressure of about 60 atm, using conventional volumetric equipment. The hydrogen uptake was 90% complete within three minutes. The amount of hydrogen absorbed was calculated by noting the change of pressure in a closed system apparatus of known volume. After this, the hydrides were quenched in liquid nitrogen and the remnant gaseous hydrogen rapidly pumped away. Mössbauer spectroscopy measurements were made at room and liquid helium temperatures using a constant acceleration spectrometer with a ^{57}Co(Rh) source. All spectra were analyzed by least squares fitting using the NORMOS program.

The magnetite-containing systems were milled in a hardened steel vial with six stainless steel balls (type 440; four of 0.25-in. diameter and two of 0.5-in. diameter) in the SPEX 8000 mixer-mill for time periods ranging from 0.5 to 17.5 hours. XRD measurements were performed using a Rigaku D-2013 diffractometer with Cu K_α radiation. Room temperature transmission Mössbauer spectra were recorded using an MS-1200 constant acceleration spectrometer equipped with a 50 mCi ^{57}Co source diffused in a Rh matrix. Least squares fitting of the Mössbauer spectra was performed with the NORMOS program.

RESULTS AND DISCUSSION

I. Nd-based intermetallics

Regarding the 2:17 compounds, Figure 1 (a) shows the room temperature transmission Mössbauer spectrum of $Nd_2Fe_{15}Si_2$ intermetallic and Figure 1 (b) represents the hyperfine magnetic field distribution extracted from this spectrum. It can be seen that this distribution exhibits three peaks, corresponding to hyperfine fields of 9, 21 and 33 T. The magnetic hyperfine field of 21 T occurs with the highest probability. The average hyperfine magnetic field calculated with this distribution is 21.74 T. The NORMOS-DIST program calculates average values for the hyperfine magnetic fields with a precision of 0.01 T for all distributions. Composition-based conclusions are thus possible with this technique.

When the $Nd_2Fe_{15}Al_2$ compound is analyzed, the distribution also exhibits three peaks, corresponding to 9, 19 and 33 T. The peak of 19 T exhibits the highest probability. The average hyperfine magnetic field for this distribution is 21.34 T. Since the average hyperfine magnetic field is proportional to the net magnetic moment, this result shows that the addition of Al tends to lower the magnetic moment in comparison with Si.

The distribution of $Nd_2Fe_{15}SiAl$ was found to have peaks at 9, 20 and 33 T, the peak at 20 T occurring with the highest probability. The average hyperfine magnetic field is 21.39 T, which is situated between the values of 21.74 T and 21.34 T obtained for $Nd_2Fe_{15}Si_2$ and $Nd_2Fe_{15}Al_2$, respectively. This confirms the previous finding that the Al substitutions tend to decrease the net magnetic moment of the sample.

The distribution pertaining to $Nd_2Fe_{15}SiMn$ has peaks at 6, 16, 20 and 33 T, the peak at 16 T having the highest probability. The fourth peak could be due to an additional nonequivalent iron site in this compound. The average value of the hyperfine magnetic field is 19.92 T, such that it

can be inferred that the addition of Mn produces a marked decrease in the net magnetic moment of the compound.

The XRD patterns of various substituted 2:17 intermetallic compounds show that only the lines of the intermetallic phase are present in the spectra, such that our systems are clearly single phased. No peaks from α-Fe or a second phase are evidenced. Moreover, it is obvious from the spectra that the majority of the intermetallic phases are in the amorphous form. This result gives further support to our Mössbauer spectra analysis based on hyperfine magnetic field distributions.

A similar treatment was applied to the 1:12 compounds. For both symmetries involved, it was found that Al and especially, Mn substitutions lower the value of the net magnetic moment, while Si additions correlate with high values of the average hyperfine magnetic field and consequently, magnetic moment.

II. Spring magnets

It can be seen from the XRD patterns of the spring magnets that the α-Fe phase is always present, while the $Nd_2Fe_{14}B$ phase is amorphous in the case of $Nd_{11}Fe_{83}B_6$ and crystalline for $Nd_{7.9}Fe_{88.1}B_4$. No other phases are present. In what follows, a detailed phase analysis was performed by Mössbauer spectroscopy.

A typical Mössbauer spectrum of annealed $Nd_xFe_{100-x-y}B_y$ alloys is shown in Figure 2. The spectrum was fitted with seven magnetic components related to two crystalline phases formed due to annealing. One sextet corresponds to the α-Fe phase with the hyperfine field, H_{hf}, of about 33 T and isomer shift, δ, of about –0.09 mm/s (in reference to the Mössbauer source), whereas others are attributed to six non-equivalent Fe sites in the $Nd_2Fe_{14}B$ structure, namely

$16k_1$, $16k_2$, $8j_1$, $8j_2$, 4c and 4e [16]. The formation of these two phases was also indicated by the x-ray diffraction results.

We further obtained the Mössbauer spectra of three alloys annealed at 750°C for 5 minutes. Very small changes in the alloy composition result in a different crystallization behavior. The spectrum of the $Nd_{11}Fe_{83}B_6$ alloy contains, besides the magnetic components, an additional paramagnetic one – a doublet with quadrupole splitting of 0.50 mm/s related to the $Nd_{1.1}Fe_4B_4$ phase, which was observed for other Nd-Fe-B alloys [17, 18]. The relative content of the paramagnetic phase is about 20%. A partial substitution of Dy for Nd causes the elimination of the paramagnetic phase; the spectrum of the $Nd_{10}DyFe_{83}B_6$ alloy consists only of the components related to the $Nd_2Fe_{14}B$ and α-Fe phases with relative abundance, A, of 93% and 7%, respectively. A similar spectrum is observed for the $Nd_{10}Fe_{85}B_5$ alloy, however, the α-Fe phase is more abundant (A=22%). This fact is apparent in the spectra by comparing the intensities of their outermost lines related to the Fe sextet.

The spectra of the $Nd_{9.3}Fe_{85.8}B_{4.9}$ alloy annealed at two different temperatures were also analyzed. The quantitative analysis of the spectral components reveals that in both cases the relative content of the α-Fe phase is close to 20%, which agrees very well with the nominal value calculated from the composition. A similar result is obtained for the $Nd_{8.5}Fe_{87.2}B_{4.3}$ alloy annealed at 715 and 726°C. However, the alloy annealed at 750°C contains less of the α-Fe phase (A=15%). This result can probably be explained by differences in the growth of the α-Fe and $Nd_2Fe_{14}B$ grains at higher annealing temperatures. The Mössbauer spectra of the $Nd_{7.9}Fe_{88.1}B_4$ alloy annealed at 715 and 726°C also show a slight decrease in the relative abundance of the α-Fe phase with increasing annealing temperature. The highest content of the α-Fe phase (about 30%) was obtained for the $Nd_{7.3}Fe_{89.1}B_{3.6}$ alloy.

By analyzing the set of experimental data one can conclude that the hyperfine field of the

α-Fe phase formed in all studied alloys is 0.2-0.7 T higher than that of the Fe foil, H_{hf}= 32.95 T. The hyperfine fields related to Fe atoms on the sites in the $Nd_2Fe_{14}B$ phase are not affected by the alloy composition. The site populations of the two phases are influenced by both the alloy composition and annealing conditions. The hyperfine parameters are not affected by the Dy addition either.

The magnetic properties of the nanocomposite magnets strongly depend on the concentration and grain size of the soft magnetic α-Fe phase [12]. An example of the influence of annealing conditions on the magnetic properties of the nanocomposite $Nd_2Fe_{14}B$/α-Fe structure is observed for the $Nd_{9.3}Fe_{85.8}B_{4.9}$ alloy. The smooth shape of the hysteresis loops is typical of an exchange-coupled system. It is known, however, that these two-phase systems reveal the exchange-coupled behavior when optimally annealed only. This is usually indicated by a highly reduced magnetization and reversible demagnetization curves [10]. The increase of the annealing temperature of the $Nd_{9.3}Fe_{85.8}B_{4.9}$ alloy from 715 ^oC to 726 ^oC causes a decrease in the magnetization, while the coercive field remains almost unchanged. This can be explained by taking into account that the sample annealed at 726 ^oC contains about 2% less α-Fe than the other one. Increasing the α-Fe concentration in the nanocomposite structure leads to the enhancement of the magnetization [12]. Hence, the annealing at 715^oC for 15 minutes seems to be more appropriate in the case of the $Nd_{9.3}Fe_{85.8}B_{4.9}$ alloy from the permanent magnet point of view.

As far as the energy product is concerned, our systems exhibit an energy product of 13±3 MGsOe (derived from the hysteresis loops), which makes these samples very competitive from the magnetic properties viewpoint.

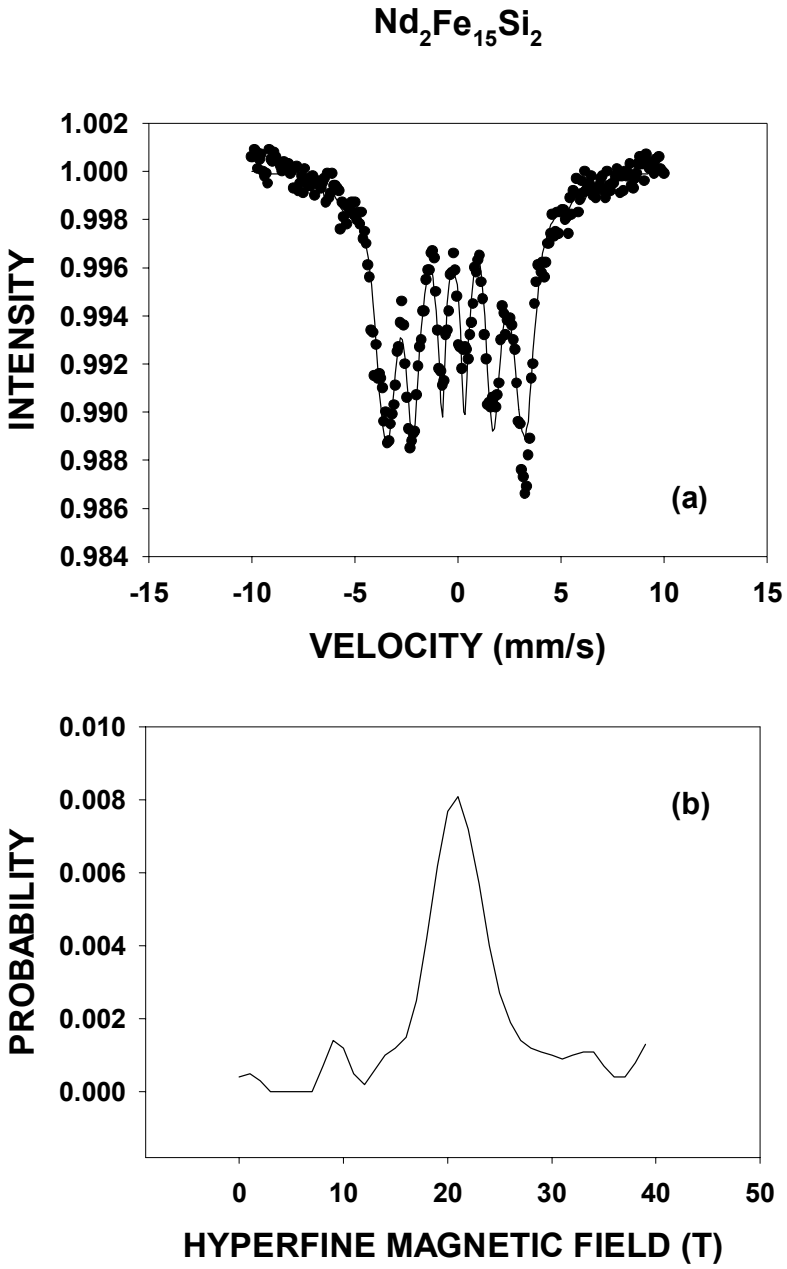
Nd2Fe15Si2
INTENSITY
1.002
1.000
0.998
0.996
0.994
0.992
0.990
0.988
0.986
0.984
-15
-10
-5
0
5
10
15
VELOCITY (mm/s)
(a)
PROBABILITY
0.010
0.008
0.006
0.004
0.002
0.000
0
10
20
30
40
50
HYPERFINE MAGNETIC FIELD (T)
(b)

FIG. 1

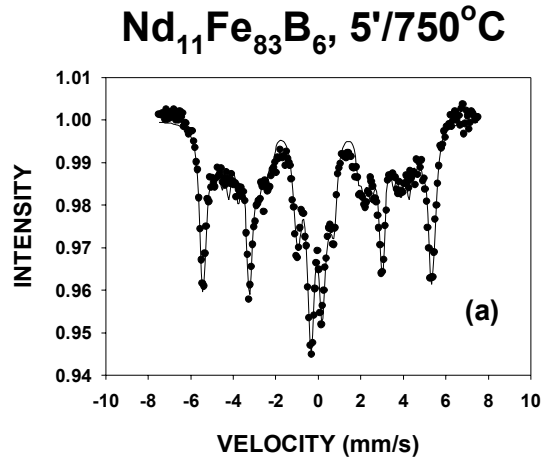
Nd11Fe83B6, 5'/750°C
INTENSITY
VELOCITY (mm/s)
(a)
Nd10DyFe83B6, 5'/750°C
INTENSITY
VELOCITY (mm/s)
(b)
Nd10Fe85B5, 5'/750°C
INTENSITY
VELOCITY (mm/s)
(c)

FIG. 2

III. Hydrogenation of iron-rich intermetallics

Figure 3 (a) shows the room temperature transmission Mössbauer spectrum of $Zr_1Cr_1Fe_1Al_{0.8}$. The spectrum could be resolved considering two quadrupole-split doublets. The first doublet has an isomer shift of -0.08 mm/s (relative to α-Fe), a quadrupole splitting of 0.61 mm/s and occupies 71.3% of the spectrum. The second doublet has an isomer shift of -0.38 mm/s, a quadrupole splitting of 0.35 mm/s and contributes 28.7% to the total spectral area. These data are consistent with Fe occupying the 2a and 6h crystallographic lattice sites in the Laves structure.

The room temperature transmission Mössbauer spectrum of the $Zr_1Cr_1Fe_1Al_{0.8}$ hydride is given in Figure 3 (b). The spectrum consists of the same quadrupole-split doublets as the spectrum in Figure 3 (a), but the doublets contribute 43.4 and 56.6% to the spectral area, respectively. It is concluded that the major effect of hydrogenation in $Zr_1Cr_1Fe_1Al_{0.8}$ is to change the relative occupancy of states in the Laves structure.

The transmission Mössbauer spectrum of $Zr_1Cr_1Fe_1Al_{0.8}$ was recorded at 4.2 K for the intermetallic system and its hydride. Both spectra were resolved considering one quadrupole-split doublet, with an isomer shift of –0.09 mm/s and a quadrupole splitting of 0.43 mm/s. These data are consistent with Fe occupying the 4f site at low temperatures. However, the linewidth increases from 0.48 mm/s before hydrogenation to 0.52 mm/s for the hydride, indicating that hydrogenation introduces a certain type of disorder in the crystalline lattice.

The room temperature transmission Mössbauer spectrum of $Zr_1Cr_1Fe_1Co_{0.8}$ and its hydride were also recorded. Both spectra were analyzed considering two quadrupole-split doublets, similar to the case of Al substitutions. The first doublet has an isomer shift of -0.08 mm/s and a quadrupole splitting of 0.61 mm/s. The second doublet has an isomer shift of -0.38 mm/s and a quadrupole splitting of 0.35 mm/s. These results are consistent with Fe occupying the 2a and 6h crystallographic lattice sites in the Laves structure, as in the case of Al substitutions. However,

the relative populations of these sites are 24.7 and 75.3% before hydrogenation and respectively, 3.5 and 96.5% after hydrogenation. It can be seen once again that hydrogenation induces changes in the site occupancy of the 2a and 6h positions, similar to the result obtained for Al substitutions. However, in the case of Co substitutions one of the sites is strongly favored with respect to the other.

The transmission Mössbauer spectrum of $Zr_1Cr_1Fe_1Co_{0.8}$ and its hydride was studied at 4.2 K. Both spectra are dominated by very weak quadrupolar interactions. The isomer shift is -0.21 mm/s in both cases, and the linewidth is 1.08 and 1.09 mm/s respectively, suggesting the presence of a distribution of inequivalent sites occupied by Fe. As in the case of Al substitutions, hydrogenation of $Zr_1Cr_1Fe_1Co_{0.8}$ correlates with the presence of a certain type of disorder in the crystalline lattice at low temperatures.

The room temperature transmission Mössbauer spectrum of $Zr_1Cr_1Fe_{1.8}$ was recorded, along with the one corresponding to its hydride. Both spectra were analyzed with a single quadrupole-split doublet, having an isomer shift of -0.3 mm/s and a quadrupole splitting of 0.25 mm/s. These results indicate that Fe occupies the 4f crystallographic sites in the Laves structure of this compound. The linewidth increases from 0.43 mm/s before hydrogenation to 0.45 mm/s for the hydride, indicating an increase in the structural disorder after hydrogenation. This result is in agreement with the previous findings on the Al and Co substituted compounds.

The transmission Mössbauer spectrum of $Zr_1Cr_1Fe_{1.8}$ and its hydride was recorded at 4.2 K. The first spectrum was analyzed considering a magnetic sextet with a hyperfine field of 9.61 T, isomer shift of -0.21 mm/s, quadrupole shift of -0.01 mm/s and a linewidth of 0.39 mm/s. The second spectrum was also analyzed with a six-line pattern, with a hyperfine magnetic field of 10.32 T, isomer shift of -0.19 mm/s, quadrupole shift of 0.034 mm/s and a linewidth of 0.45 mm/s. The increase in the hyperfine magnetic field after hydrogenation indicates the presence of a weak

ferromagnetism in the Laves structure, while the increase in the linewidth suggests a more pronounced crystalline disorder in the lattice.

IV. Mechanochemical activation of magnetite-containing systems

a) Mechanochemical activation of Fe_3O_4+Fe

We subjected a mixture of magnetite and iron (80-20 wt %) to high-energy ball milling for time periods ranging from 0.5 to 14 hours. The XRD patterns of these systems were recorded. The spectra are consistent with the partial transformation of magnetite and iron to hematite after 10 hours of milling.

The room temperature transmission Mössbauer spectra of the Fe_3O_4+Fe mixture, corresponding to samples milled for 0.5, 1 and 14 hours, respectively were obtained. The first spectrum was analyzed considering three sextets, corresponding to Fe and the tetrahedral and octahedral sublattices of magnetite. The second and third spectra were fitted with an additional sextet, corresponding to the appearance of hematite in the milled systems. The magnetic hyperfine field values obtained for the tetrahedral and octahedral sublattices were typical for magnetite. One striking feature was the linewidth of the octahedral sublattice in the range 0.97 to 2.04 mm/s, which indicates that the milling-induced phase transformations are initiated with a dramatic disorder of the octahedral sublattice. The initial amount of Fe (20.97 %) determined from the Mössbauer spectra is in perfect agreement with the original composition of the mixture. The dependence of the abundance of phases on the time of ball milling was studied. The percentage of hematite produced in the reaction increased from 0 to 44.1 % after the first 10 hours of mechanochemical activation, while the content of magnetite decreased from 79.03 % to

51.56 % and the amount of Fe dropped to 4.34 %. The reaction can be used to obtain nanometer-size magnetite by ball milling, due to the inhibition of its transformation to hematite, caused by the presence of iron atoms.

b) Mechanochemical activation of Fe_3O_4:Co^{2+}

We exposed the system $Fe_{3-x}Co_xO_4$ (x=0.1) to ball milling for time periods from 2.5 to 17.5 hours and extended up to 50 hours. The XRD patterns are given in Figure 4. The spectra indicate that the cobalt-doped magnetite is converted to hematite even after 15 hours of ball milling. The most important feature in these XRD spectra is the absence of the Co lines from the patterns. This result indicates that the Co^{2+} ion is not kicked out of the lattice during the milling-induced phase transformations, but remains in the crystalline lattice, giving rise to a cobalt-doped hematite.

The room-temperature transmission Mössbauer spectra of the Fe_3O_4:Co^{2+} samples, milled for time periods of 2.5, 5 and 17.5 hours were analyzed. All spectra were fitted with three sextets, corresponding to cobalt-doped hematite and to the tetrahedral and octahedral positions of cobalt-doped magnetite. The linewidth of the octahedral sextet was found to be in the range 0.74 to 1.19 mm/s, fact which demonstrates that the mechanochemical activation process starts with the destruction of the octahedral magnetic sublattice of the cobalt-doped magnetite. The linewidth of the hematite sextet is also broadened (0.38 mm/s) and this result is consistent with the presence of cobalt atoms in the hematite lattice. The phase populations were studied as function of the ball milling time. It was observed that the amount of cobalt-doped hematite formed increased from 12.72 % after 2.5 hours to 56.67 % after 17.5 hours of ball milling, while the amount of cobalt-doped magnetite decreased from 87.28 % to 43.33 % during the same time

interval. This experiment is important because the Co ion, introduced as a spy in the crystalline lattice of magnetite, was demonstrated to remain in the crystalline lattice and undergo the phase transformation inside hematite.

c) Mechanochemical activation of Fe_3O_4+Co

We prepared a mixture of Fe_3O_4 and Co powders (80-20 wt %) and subjected it to ball milling for time periods ranging from 0.5 to 6 hours. The XRD patterns were consistent with the formation of cobalt ferrite (a strongly cobalt-substituted magnetite) even after 4 hours of milling exposure. The transformation occurs with the intermediate formation of hematite, which is present in the system during the first four hours of mechanochemical activation.

The room-temperature transmission Mössbauer spectra corresponded to milling times of 0.5, 4 and 10 hours, respectively. The first two spectra were analyzed considering three sextets, corresponding to hematite and the two sublattices of magnetite. The third spectrum, however, was fitted with only two sextets, with the hyperfine parameters corresponding to the tetrahedral and octahedral sublattices of cobalt ferrite, $CoFe_2O_4$. It can be seen once again from these values that the large linewidth of the octahedral sublattice (1.52 to 2.14 mm/s) indicates that the disorder at these sites is the precursor for the milling-induced phase transformations. The Mössbauer data are in agreement with the XRD results and support the formation of cobalt ferrite, with the intermediate occurrence of hematite in this system. The phase fractions were investigated as functions of ball milling time. It was observed that the amount of hematite exhibits a maximum for a milling time of 2 hours, followed by a decrease to zero, concurrent with the formation of cobalt ferrite in the system. This experiment demonstrates that ball milling can be successfully used to synthesize the cobalt ferrite phase.

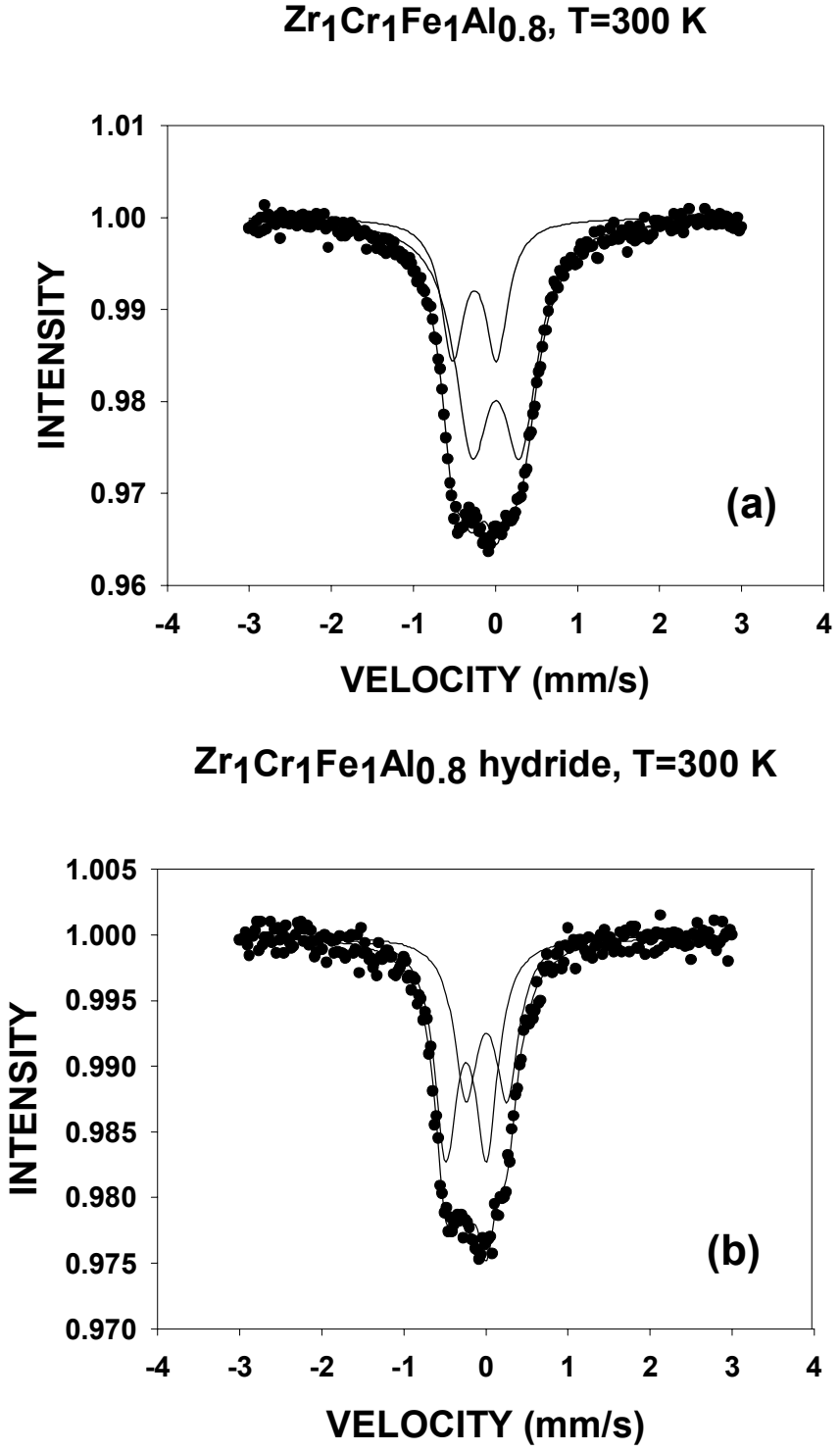
Zr1Cr1Fe1Al0.8, T=300 K
INTENSITY
1.01
1.00
0.99
0.98
0.97
0.96
-4
-3
-2
-1
0
1
2
3
4
VELOCITY (mm/s)
(a)
Zr1Cr1Fe1Al0.8 hydride, T=300 K
INTENSITY
1.005
1.000
0.995
0.990
0.985
0.980
0.975
0.970
-4
-3
-2
-1
0
1
2
3
4
VELOCITY (mm/s)
(b)

FIG. 3

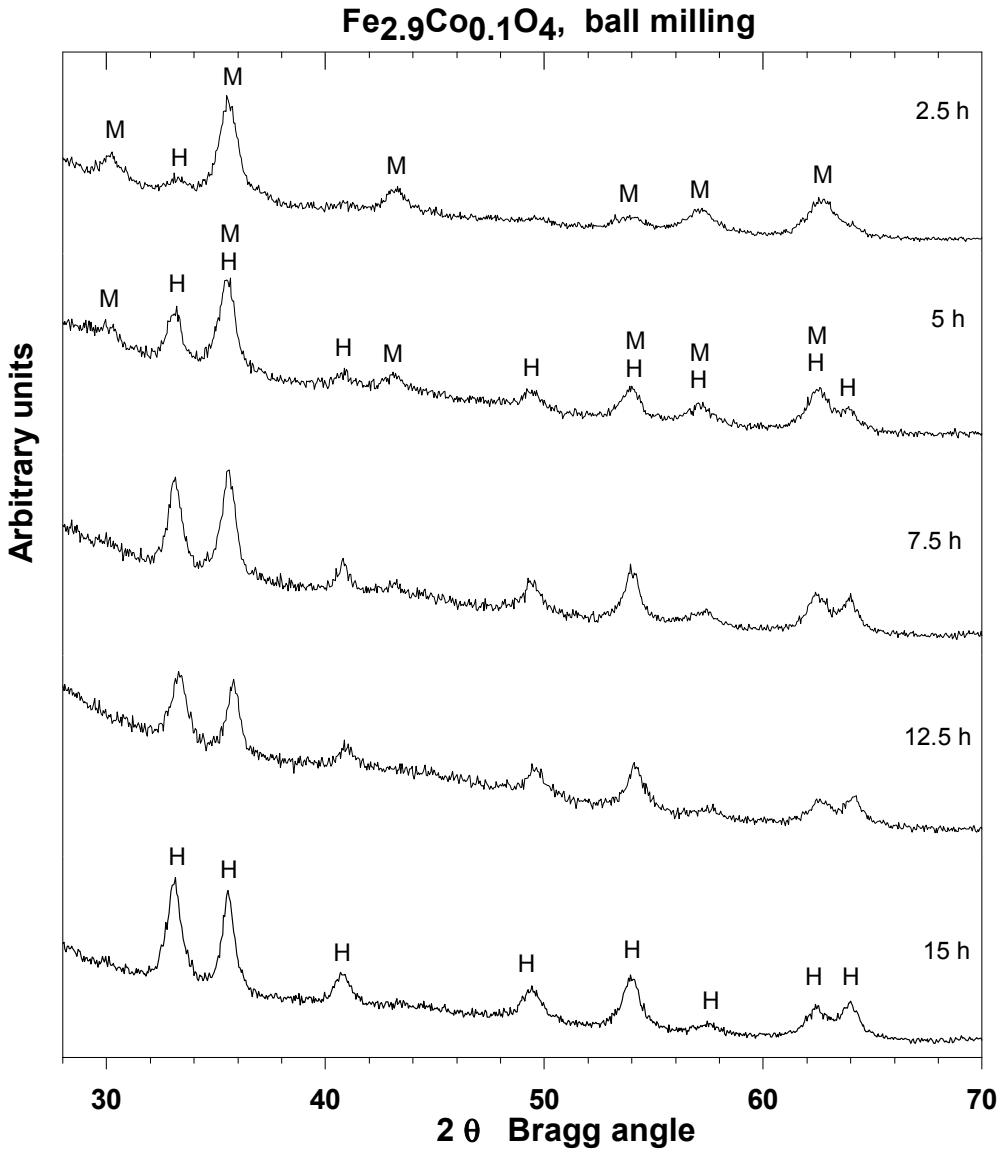
Fe2.9Co0.1O4, ball milling
Arbitrary units
2.5 h
5 h
7.5 h
12.5 h
15 h
M
H
30
40
50
60
70
2 θ Bragg angle

FIG. 4

CONCLUSIONS

We prepared and characterized by Mössbauer spectroscopy and XRD several intermetallic compounds of the type 2:17 and 1:12 in order to investigate the effect of various substitutions on the hyperfine magnetic fields. For both symmetries involved, it was found that Al and especially, Mn substitutions lower the value of the net magnetic moment, while Si additions correlate with high values of the average hyperfine magnetic field and consequently, magnetic moment.

The influence of annealing conditions on the microstructure of the Nd-Fe-B alloys was studied as a function of their composition and annealing conditions. Mössbauer spectroscopy allowed us to identify the formed phases as well as to determine their hyperfine fields and relative abundance in the nanocomposite material. In all alloys the $Nd_2Fe_{14}B$ and α-Fe phases were formed due to annealing. However, in the case of the $Nd_{11}Fe_{83}B_6$ alloy with the highest Nd content a significant amount of the $Nd_{1.1}Fe_4B_4$ paramagnetic phase was observed. In the studied set of alloys the highest fraction of the α-Fe phase (about 30%) was obtained for the $Nd_{7.3}Fe_{89.1}B_{3.6}$ alloy. The formation of the exchange coupled material was checked by hysteresis loop measurements at room temperature in all cases.

Our detailed Mössbauer spectroscopy investigation of the $Zr_1Cr_1Fe_1T_{0.8}$ and its hydrides, with T=Al, Co and Fe demonstrates the microscopic effects associated with the process of hydrogenation in these intermetallic compounds. The effects range from modification of the site populations and inducing crystallographic disorder to weak ferromagnetism and enhancement of the hyperfine magnetic field.

Finally, our XRD and Mössbauer results obtained on three magnetite-containing systems demonstrate that the presence of iron can partially inhibit the transformation of magnetite to hematite, that cobalt ions in magnetite remain in the crystalline lattice during the milling-induced

phase transformations and that mechanochemical activation can be successfully used to synthesize new magnetic phases, such as cobalt ferrite.

REFERENCES

1.M. Sorescu, A. Grabias, M. Valeanu, Intermet. 9 (2001) 67

2.M. Rosenberg, R.J. Zhou, M. Katter, L. Schultz, G. Filoti, J. Appl. Phys. 73 (1993) 6035

3.W.B. Yelon, Z. Hu, M. Chen, H. Luo, P.C. Ezekwenna, G.K. Marasinghe, W.J. James, K.H.J. Buschow, D.P. Middleton, F. Pourarian, IEEE Trans. Magn. 32 (1996) 4431

4.X. Chen, Z. Altounian, D.H. Ryan, J. Magn. Magn. Mater. 125 (1993) 169

5.N. Plugaru, M. Morariu, A. Galatanu, D.P. Lazar, D. Barb, J. Appl. Phys. 82 (1997) 6193

6.H. Luo, Z. Hu, W.B. Yelon, P.C. Ezekwenna, G.K. Marasinghe, W.J. James, IEEE Trans. Magn. 32 (1996) 4389

7.J.F. Herbst, J.J. Croat, R.W. Lee, J. Appl. Phys. 53 (1982) 250

8.G.J. Long, G.K. Marasinghe, S. Mishra, O.A. Pringle, F. Grandjean, K.H.J. Buschow, D.P. Middleton, W.B. Yelon, F. Pourarian, O. Isnard, Solid State Commun. 88 (1993) 761

9.R. Coehoorn, D.B. de Mooij, J.P.W.B. Duchateau, K.H.J. Buschow, J. Phys. (Paris) Colloq. 49 (1998) C8-669

10.E.F. Kneller and R. Hawig, IEEE Trans. Magn. 27 (1991) 3588

11.A. Manaf, R.A. Buckley, H.A. Davies, J. Magn. Magn. Mater. 128 (1993) 302

12.J. Bauer, M. Seeger, A. Zern, H. Kronmüller, J. Appl. Phys. 80 (1996) 1667

13.J. Ding, Y. Li, K.Y. Lee, J. Phys.: Condens. Matter 10 (1998) 9081

14.T. Kobayashi, M. Yamasaki, M. Hamano, J. Appl. Phys. 87 (2000) 6579

15.Y.Q. Wu, D.H. Ping, K. Hono, M. Hamano, A. Inoue, J. Appl. Phys. 87 (2000) 8658

16.H. Onodera, A. Fujita, H. Yamamoto, M. Sagawa, S. Hirosawa, J. Magn. Magn. Mater. 68 (1997) 6

17.Z.H. Cheng, B.G. Shen, M.X. Mao, J.J. Sun, Y.D. Zhang, F.S. Li, Phys. Rev. B 52 (1995) 9427

18.M.M. Raja and A. Narayanasamy, J. Appl. Phys. 84 (1998) 5715

19.S. Hirosawa, F. Pourarian and W.E. Wallace, J. Magn. Magn. Mater. 43 (1984) 187.

20.F. Pourarian and W.E. Wallace, J. Solid State Chem. 55 (1984) 181.

21.F. Fujii, F. Pourarian and W.E. Wallace, J. Magn. Magn. Mater. 27 (1982) 215.

22.H. Fujii, V.K. Sinha, F. Pourarian and W.E. Wallace, J. Less-Common Met. 85 (1982) 43.

23.L.Y. Zhang, A.T. Pedziwiatr, F. Pourarian and W.E. Wallace, J. Magn. Magn. Mater. 68 (1987) 309.

24.M. Sorescu and M. Valeanu, J. Appl. Phys. 87 (2000) 6725.

25.Ref. 1.

26. M. Sorescu and A. Grabias, Intermet. 10 (2002) 317.

27.L. Schultz, K. Schnitzke, J. Wecker, M. Katter and K. Kuhrt, J. Appl. Phys. 70 (1991)6339.

28.Y. Liu, M. P. Dallimore, P.G. McCormick and T. Alonso, Appl. Phys. Lett. 60 (1992) 3186.

29.G. Herzer, IEEE Trans. Magn. 25 (1989) 3327.

30.M. Sorescu, A. Grabias, L. Diamandescu and D. Tarabasanu, J. Mat. Synth. Proc. 8 (2000) 67.

31.M. Sorescu, D. Tarabasanu-Mihaila and L. Diamandescu, J. Mat. Synth. Proc. 7 (1999) 167.

32.C. C. Koch, Ann. Rev. Mat. Sci. 19 (1989) 121.

33.L. Schultz, J. Less-Common Met. 145 (1988) 233.

34.H. J. Fecht, E. Hellstern, Z. Fu and W. L. Johnson, in *Advances in Powder Metallurgy* (Metal Powder Industries Federation, Princeton, NJ, 1989) Vols. 1-3, pp. 111-122.

35.M. Pardavi-Horvath and L. Takacs, J. Appl. Phys. 73 (1993) 6958.

36.E. Bonetti, L. Del Bianco and S. Signoretti, J. Appl. Phys. 89 (2001) 1806.

37.E. Petrovsky, M. D. Alcala, J. M. Criado, T. Grygar, A. Kapicka and J. Subrt, J. Magn. Magn. Mater. 210 (2000) 257.

LIST OF ACRONYMS AND ABBREVIATIONS

XRD=X-ray diffraction

LIST OF PUBLICATIONS

1. M. Sorescu, M. Valeanu and L. Diamandescu, "Effect of substitutions on the hyperfine magnetic field in Nd-based intermetallics", Intermetallics, accepted for publication.

2. M. Sorescu, A. Grabias and M. Valeanu, "Structure and properties of spring magnets", IEEE Transactions on Magnetics, accepted for publication; oral presentation at the INTERMAG Conference in Boston, MA on March 29-April 3, 2003.

3. M. Sorescu, F. Pourarian and R.A. Brand, "Mössbauer study of hydrogenation effects in iron-rich intermetallics", Journal of Materials Science Letters, submitted for publication.

4. M. Sorescu, L. Diamandescu and A. Grabias, "Kinetics of phase transformations by mechanochemical activation in magnetite-containing systems", Journal of Materials Science, submitted for publication.